Structural Insight Into Aeromonas Hydrophila AHL Synthase AhyI Driving Acyl-ACP Selective Recognition

Lei Jin
Ningbo University
Yu chen
Zhejiang Marine Fisheries Research Institute
Wenge Yang (yangwenge_nbu@126.com)
Ningbo University

Research Article

Keywords: Aeromonas hydrophila, N-acyl-homoserine lactone, AhyI, biosynthesis, Enzyme kinetics, Substrate recognition, Structural basis

Posted Date: April 14th, 2021

DOI: https://doi.org/10.21203/rs.3.rs-403119/v1

Abstract

Background: The gram-negative bacterium *Aeromonas hydrophila* as the major causative agent of the fish disease motile aeromonad septicemia, uses N-acyl-homoserine lactone quorum sensing signals to coordinate biofilm formation, motility and virulence gene expression in pathogens. Thus, AHL signaling pathway is considered as a therapeutic target against pathogenic *A. hydrophila* infection. AHL autoinducers biosynthesis in *A. hydrophila* are specifically catalyzed by an ACP-dependent AHL synthase AhyI using SAM and acyl-ACP as the precursors. Our previously reported AhyI protein heterologously expressed in *E. coli* strain showed the production characteristics of medium-long chain AHLs, although AhyI was only considered as a short-chain C_4/C_6-HSL synthase during the past two decades.

Results: In this study, we carried out the in vitro biosynthetic assays of six AHL molecules and kinetic studies of recombinant AhyI with a panel of four linear acyl-ACPs. These resulting data all indicate that C_4/C_6-ACP are the native acyl substrates for AhyI against acyl-ACPs with longer linear chains as the non-native acyl donor. In an effort to further understand AhyI acyl-donor substrates preferences, we performed a structural comparison of three ACP-dependent LuxI homologs (TofI, BmaI1 and AhyI), and identified three key hydrophobic residues (I67, F125 and L157) as part of the acyl-chain binding pocket that confer AhyI to selectively recognize native C_4/C_6-ACP substrates. The predictions were further supported by computational Ala mutation assay.

Conclusions: Our current studies redefined AhyI protein that is a multiple short- to long-chain AHL molecules synthase with longer acyl-ACPs (C8~C14) as the non-native substrates, and we also theorized that with knowledge of the key residues in AHL signal synthase AhyI to drive acyl-ACP selective recognition.

Background

The opportunistic pathogen *Aeromonas hydrophila* is a ubiquitous inhabitant of various aquatic environments worldwide and infects fish, reptiles, amphibians, and mammals, including humans [1, 2]. In particular, motile aeromonad septicemia (MAS) caused by *A. hydrophila* has become the most important bacterial disease in fish species, and frequent outbreaks lead to huge economic losses periodically per year [3, 4]. To date, antibiotics usually are the first prevention and treatment for *A. hydrophila* infections, but the extensive use of antibiotics leads to the development of multidrug resistance [5].

Many Gram-negative bacteria use autoinducers as signal molecules to alter specific genes expression for enabling population density control termed quorum sensing (QS) [6, 7]. N-acyl-homoserine lactones (AHLs), the best characterized QS signals, are wide distributed in most gram negative bacteria [8]. AHL molecules possess conservative homoserine lactone ring (HSL), but vary in acyl chain length from C_4 to C_{18}, in backbone branch or unsaturation and decoration (i.e., 3-oxo or 3-OH substitution at the β-carbon) [9]. AHL quorum sensing has been implicated as an important factor to affect the virulence in some bacterial pathogens [10]. For example, AHL-based QS enhances the biofilm maturation, modulates the

exoenzymes and hemolysin production and is involved in the regulation of type III and type secretion system in the zoonotic agent *A. hydrophila* [11-14]. Importantly, targeting AHL signaling circuit asserts less selective pressure for developing drug resistances, and is therefore considered as an alternative strategy of antibiotic usage to provide protection against *A. hydrophila* that depends on QS to initiate pathogenic expression (Fig. 1).

The LuxI family known as major AHL synthases act as signal initiator proteins to synthesize specific N-acyl-homoserine lactones [15]. The LuxI proteins functioned as AHL synthases by utilizing precursors S-adenosyl-L-methionine (SAM) as the amino donor and acyl-acyl carrier protein (acyl-ACP) / acyl-Coenzyme A (acyl-CoA) as an acyl donor [16-18]. Both acyl-ACP- and acyl-CoA-dependent AHL synthases undergo acylation and lactonization to synthesize AHL and release methylthioadenosine (MTA) via an acyl-SAM intermediate [19-21]. SAM is a conserved substrate for all AHL synthases, and yet specificity for the AHL signals derives from the acyl chain of acyl-ACP or acyl-CoA substrates [22, 23].

The crystal structures of three LuxI members known as ACP-dependent AHL synthases have been resolved, including *Pseudomonas aeruginosa* LasI (PDB Code: 1RO5) [24], *Pantoea ste*wartii EsaI (PDB Code: 1KZF) [21] and *Burkholderia glumae* TofI (PDB Code: 3P2F) [25]. In addition, several cocrystal structures of complexes with various ligands and a CoA-dependent AHL synthase BjaI from *Bradyrhizobium japonicum* were also identified recently [19]. These LuxI-type AHL synthases exhibited a similar α-β-α fold with a V-shaped cleft and a prominent active-site cavity, reveal a detectable structural similarity to the GCN5-related N-acetyltransferases (GNATs) family [26]. The site-specific variants LuxI suggest that some identified crucial residues play integral roles in catalysis, and establish structural basis for substrate specificity. AHL synthase specificity is tight but not absolute, likely affected from cognate acyl-ACP pool supply [27]. For example, a C_8-HSL synthase *Burkholderia mallei* BmaI1 can utilize non-native acyl-ACP substrates from the *E. coli* acyl-ACP pool to synthesize nonspecific AHLs, although the catalytic efficiencies are lower than with the native octanoyl-ACP (C_8-ACP) [28]. Currently, the general features of molecular structure that determine substrate selectivity in partial LuxI-type AHL synthase are clear, but many details for other well-recognized AHL synthases (e.g. AhyI) remain to be defined.

AHL molecules in *A. hydrophila* are typically produced by the LuxI homolog AhyI and perceived by the AhyR receptors [29]. For a long time past, *A. hydrophila* AhyI was only identified as a short-chain AHLs (C_4-HSL and C_6-HSL) producer [30]. However, our recent work showed that the recombinant AhyI protein expressed in *E. coli* can synthesize six types of AHLs, namely, C_4-HSL, C_6-HSL, C_8-HSL, C_{10}-HSL, C_{12}-HSL, and C_{14}-HSL [31]. Due to a lack of in vitro biosynthetic assays of medium- and long-chain AHLs by AhyI, there is not any substantial evidence yet to support whether or not the longer-chain AHLs observed in the heterologous expression strain was an artifact. In this paper, we presented kinetic studies of AhyI with multiple acyl-ACP substrates derived from recombinant *E. coli* to verify this hypothesis as longer acyl-ACPs might be the acyl substrates for AhyI. Moreover, we propose new insights into the acyl-donor substrates preferences and the structural determinants of substrate specificity for AhyI.

Methods

Reagents and strains

The AHL standards purchased from Sigma-Aldrich Chemical Co. were dissolved in methanol to prepare 100 μM stock solutions. Chemicals for protein preparation and enzyme assays were purchased from Sangon Biotech (Shanghai) Co., Ltd., Bio-Rad Laboratories (Shanghai), Inc. or Sigma-Aldrich. The 6x His-Tag Protein Purification Kit and BCA Protein Assay Kit were from ProbeGene Inc. (Xuzhou, China). Molecular biology reagents used for construction of cloning vectors were from Sangon Biotech. UPLC-MS/MS solvents and other conventional reagents were from Merck KGaA (Germany) or Sinopharm Chemical Reagent Co., Ltd. (Shanghai, China). All primers and oligonucleotides for PCR were purchased from Sangon Biotech.

The pET-His plasmids carrying the genes for *Escherichia coli* MG1655 ACP, *Vibrio harveyi* B392 AasS, and *A. hydrophila* HX-3 AhyI were supplied by our previous work [31]. The pBAD plasmid (no His-tag) carrying *E. coli* ACPs was obtained as a kind gift from Prof. Haihong Wang at the South China Agricultural University, Guangzhou. *E. coli* BL21(DE3) for protein overexpression were grown on LB at 37 ℃.

Purification of holo-ACP

The plasmids pET28a-*acpP* and pBAD-*acpS* were transformed into *E. coli* BL21 (DE3) together, and positive clones were screened on LB medium containing kanamycin (50 μg/mL) and chloramphenicol (25 μg/mL). *E. coli* strain carrying plasmids pET28a-*acpP* and pBAD-*acpS* was cultured at 37 ℃ with shaking in 2 L of LB media supplemented with 0.1 mM L-arabinose and the same concentrations of antibiotics [37]. The culture was grown to an optical density of 0.8, and then induced by the addition of 0.5 mM isopropyl-β-D-thiogalactopyranoside (IPTG) followed by incubation for an additional 4 h. Cell pellets were harvested by centrifugation at 10000 rpm for 10 min at 4 °C and washed twice with equal volume of 20 mM Tris-HCl (pH 8.0). Cells were then resuspended in 10 mL ice-cold buffer A containing 20 mM Tris-HCl pH 8.0, 10 mM $MgCl_2$ and 5 mM DTT, and lysed by sonication. Cell debris was removed by centrifugation at 10000 rpm for 20 min at 4 °C, 1 mM CoA was added to the supernatant and incubated for 4 h at 37 °C. An equal volume of ice-cold isopropanol was added to the extract and incubated with stirring at 4 °C for 1 h to remove most other proteins. Following centrifugation, the supernatant was concentrated under nitrogen to the half-volume and then dialyzed overnight against a buffer of 50 mM 2-(N-morpholino) ethanesulfonic acid (MES), pH 6.1. The dialyzed extract was cleared by centrifugation, and the supernatant was applied to a Ni-IDA column. The column was sequentially washed with 100 ml of buffer B (20 mM Tris-HCl pH 8.0, 2 M NaCl and 0.1% TritonX-100), 20 ml of buffer C (20 mM Tris-HCl pH 8.0, 50 mM NaCl and 0.1% TritonX-100) and 50 ml of 10 mM imidazole in buffer C. Holo-ACP with a C-terminal 6×His-tag was eluted from the column using appropriate volumes of buffer C with 250 mM imidazole. The nickel ions and imidazole were efficiently removed from the ACP solution after dialysis twice against buffer D (20 mM Tris-HCl pH 8.0, 5 mM DTT). Purified holo-ACP proteins were concentrated to a volume of 4 mL and the final concentration was quantified by Nanodrop UV-Vis analysis using a molar extinction

coefficient of 1.8×10^3 at 280 nm [38]. The purity of the holo-ACP was monitored by using conformationally sensitive gel electrophoresis on a non-denaturing 17.5% polyacrylamide gel containing 2.5 M urea (urea-PAGE) based on the method described previously [33].

Preparation of acyl-ACP substrates

Vibrio harveyi AasS was utilized to synthesize the linear acyl-ACPs (C_4~C_{14}) [39]. A reaction mixture contained 100 mM Tris-HCl (pH 7.8), 10 mM $MgCl_2$, 5 mM DTT, 10 mM ATP, 100 μM fatty acid, 20 μM holo-ACP and 0.75 μM purified AasS and was incubated at 37 °C for 4 h. Notably, the additional reaction times (more than 12 hours) were required for the C_4-ACP, C_{12}-ACP and C_{14}-ACP preparation. The reaction was stopped by addition of 50 % ice-cold isopropanol to remove AasS protein. This suspension resulting from centrifugation was treated with two volumes of acetone to precipitate acyl-ACP proteins and stayed at -20 °C overnight [40]. Following centrifugation and two washes with three volumes of acetone, the precipitates were air dried and resuspended in buffer D. Essentially complete conversion to acyl-ACPs were verified by urea-PAGE.

In vitro assay of AhyI activity

The acyl substrate recognition profiles of AhyI was analyzed using the reaction mixture (0.5 mL) containing 100 mM Tris-HCl (pH 7.8), 1 mM SAM and 100 μM acyl-ACP (C_4~C_{14}). Reactions were initiated by the addition of 1 μM purified AhyI and then incubated at 37 °C for 60 min. The AHL products in the reaction mixtures were extracted twice with an equal volume of ethyl acetate containing 0.01% glacial acetic acid. The organic phase was dried with a nitrogen gun and residues were dissolved in 1.0 mL of methanol. The final products were validated by ultraperformance liquid chromatography-tandem mass spectrometry (UPLC-MS/MS) analysis according to the method described previously [31].

To determine the kinetic parameters for AhyI, the enzymatic reaction was monitored using a colorimetric assay that measured the decrease in 2,6-dichlorophenolindophenol (DCPIP) absorbance at 600 nm [23, 41]. The typical reaction contained 30 μM DCPIP, 100 mM Tris-HCl (pH 7.8), 1 mM SAM, and 2-300 μM acyl-ACP. Following a 10 min incubation period, the reactions were then initiated by AhyI addition. AhyI was maintained at 0.75 μM for C_4-ACP and C_6-ACP, or 1 μM for C_8-ACP and C_{10}-ACP. The reduction of DCPIP by free holo-ACP released in AHL synthesis was monitored at 600 nm ($\Delta\varepsilon_{600}$ = 21,000 $M^{-1}cm^{-1}$) over 10 min and initial rates were calculated based on the progress curve. To estimate kinetic constants, the initial rate data were fitted to Michaelis-Menten or substrate inhibition equation using the Graphpad Prism 8.0.

Molecular docking

The homology model of AhyI was generated using the program Modeler v9.19 with TofI structure (PDB code: 3P2F) as the molecular template. The detailed method for model construction and refinement was described in our previous publication [31]. The initial structures of mutated AhyI (I67A, F125A and L157A) were prepared using PyMOL 1.8, following by energy optimization to allow the mutant structure to find

the minimum energy conformation. The structures of acyl-4'-phosphopantetheine (C_4-, C_6-, C_8-, C_{10}-, C_{12}- and C_{14}-4'-PP) were processed with AutoDock Tools 1.5.6 by adding hydrogens, and further optimized using the PM3 Hamiltonian in MOPAC program. Molecular docking of acyl-4'-PP with AhyI was carried out by AutoDock 4.2.6 program [42]. The grid box was set up with 60×50×60 points in the XYZ axes at a grid spacing of 0.375 Å. The number of Genetic Algorithm (GA) run was set to 100, and the default settings were used for the rest parameters. Finally, the optimal 3D docking conformations with lowest energy scoring were selected for computational Ala mutation assay. The binding affinity values from three parallel dockings of each protein-ligand were collected for further statistical analysis.

Results

Synthesis of acyl-ACP substrates

Overexpressed ACP in *E. coli* carrying plasmid pET28a-*acpP* was generally isolated primarily in the apo-form. Apo-ACP must undergo 4’-phosphopantetheine (4’-PP) modification of the conserved Ser36 through a phosphodiester bond to form active holo-ACP, and then fatty acids can be bound in thioester linkage to the 4’-PP group thiol (Fig. S1) [32]. In the present study, *E. coli* strain carrying plasmid pET28a-*acpP* was additionally transformed with the plasmid pBAD-*acpS* expressing the *E. coli* AcpS which transfers 4’-PP from CoA to apo-ACP. The phosphopantetheinylation of apo-ACP was shown to be complete by urea-PAGE analysis (Fig. S2). Then, the purified *Vibrio harveyi* acyl-ACP synthetase (AasS) was used to catalyze reaction of holo-ACP and free fatty acids yielding the linear acyl chain of ACP substrates. The reaction products were also analyzed by urea-PAGE (Fig. S2). No single holo-ACP bands on polyacrylamide gel were obtained, indicating that each reaction of acyl-ACP biosynthesis was completed. Although the molecular weight of the hexahistidine tagged ACPs are higher than native forms, the synthetic acyl-ACPs with C-terminal His-tags remain active but at somewhat less levels than the native protein. For subsequent enzymatic analysis, the activity of hexahistidine tagged acyl-ACPs will be sufficient.

Analysis of acyl-ACP utilization pools

Prior UPLC-MS/MS analysis of metabolites from cultured supernatants of recombinant *E. coli* carrying pET30a-*ahyI* demonstrated production of six AHL signals. To further verify the in vitro enzymatic activity of AhyI, we tested a panel of linear acyl-ACP (C_4~C_{14}-ACP) and SAM as substrates for the formation of the corresponding AHL. Six typical characteristic peaks in total ion current (TIC) chromatograms were observed respectively by UPLC-MS/MS analysis, consistent with the retention times of the AHL standards (Fig. 2). Moreover, all corresponding ion peaks for respective C_4-HSL (*m/z* 172), C_6-HSL (*m/z* 200), C_8-HSL (*m/z* 228), C_{10}-HSL (*m/z* 256), C_{12}-HSL (*m/z* 284), and C_{14}-HSL(*m/z* 312) along with the precursor ion peak (*m/z* 102) matched those of the AHL synthetic standards in our previous experiments [31], and mass data were shown in Fig. 3. These data suggest that AhyI can use these linear acyl substrates to synthesize the AHL products, including the short-chain C_4/C_6-HSLs and the medium-chain C_8/C_{10}-HSLs,

as well as the long-chain C_{12}/C_{14}-HSLs. Thus, the in vitro experiments confirmed the conclusion that acyl-ACPs with longer linear chains than C6 were also the acyl-donor substrates for AhyI.

Kinetics of AHL synthesis by AhyI

The kinetic analyses for AhyI against four linear acyl-ACPs (C_4~C_{10}-ACP) were performed using a DCPIP colorimetric method. Under fixed SAM conditions, the kinetic parameters for AhyI using each of the acyl-ACPs as an acyl-donor substrate are described in Table 1. The AhyI enzyme is clearly in favor of C_4-ACP with the lowest K_m (1.85×10^{-6} M) and the highest k_{cat}/K_m (12.29×10^3 $M^{-1}s^{-1}$) values. Catalytic efficiency was severely affected as the acyl chain length increased. For C_6-ACP, the k_{cat}/K_m values decreased more than 8-fold compared to C_4-ACP. However, AhyI shows 62-fold and 175-fold lower catalytic efficiencies in response to C_8-ACP and C_{10}-ACP, indicating enzyme activity could be significantly inhibited when the length of acyl chains is C8 or longer. These data are in agreement with in vivo observations that the C_4-HSL with highest abundance and other AHL signals with much lower abundance were found in the recombinant *E. coli* and *A. hydrophila* strains [31]. It is worth mentioning that catalytic efficiencies were extremely low at less than 500 μM concentration of C_{12}/C_{14}-ACP substrates (data not shown). On the other hand, highly concentrated C_{12}/C_{14}-ACP proteins were prepared with great difficulty due to solubility issues with long-chain fatty acids (or salt) during the AasS reaction. Finally, we failed to conduct the kinetic studies for these two acyl substrates with AhyI when the fixed substrate was SAM.

Discussion

In contrast to many studies using *E. coli* DK574, DK574-pJT93 or DK574-pJT94 to prepare holo-ACP [19, 28, 33], the *E. coli* holo-ACP expression system in this study is easily conducted and the soluble holo-ACP with a hexahistidine tag could be routinely purified by Ni^{2+} affinity chromatography in most laboratories. Normally the unmodified apo-ACP accumulation will strongly inhibit growth of *E. coli* [34]. However, our results indicated that overproduction of *E. coli* ACP therefore appeared to no directly impact strain growth, which was attributed to the overexpression of holo-ACP synthase AcpS, resulting in a rapid alteration of apo- to holo-ACP. For the acyl-ACP biosynthetic methods apart from AasS pathway, the phosphopantetheinyl transferase of Sfp from *Bacillus subtilis* to transfer the acyl-phosphopantetheine moiety of acyl-CoA to apo-ACP is also commonly used in the acyl-ACP synthesis [35]. However, compared to the two enzymatic methods, the acyl-ACP biosynthetic pathway in the present study could be more economical due to the high price and incomplete commercial supply of acyl-CoA products.

Notably, the substrate-velocity curves were hyperbolic for C_4/C_6-ACP and sigmoidal for C_8/C_{10}-ACP (Fig. 4). Interestingly, AhyI with C_4-ACP utilization displayed a substrate inhibition property, which has also been observed for other LuxI type AHL synthases (e.g. BjaI and BmaI1) [19, 28]. Prior kinetic studies on the BmaI1 established that hyperbolic behavior was appropriate for native acyl-ACP substrates with high reaction rates, while non-native acyl-ACPs reacting with BmaI1 showed sigmoidal response in rate curves [28]. Based on the above theory, our kinetic data suggest that C_4/C_6-ACP are the native acyl-donor

substrates for AhyI and others are considered as non-native acyl-ACPs. Thus, it is reasonable to assume that the short-chain C_4/C_6-HSL are the specific (native) AHL products for the AHL synthase AhyI, and nonspecific medium- and long-chain AHLs with low synthesis rates could disrupt intercellular communication. However, the AHL-dependent regulation in *A. hydrophila* involving the medium- and long-chain AHLs have not been reported, and quorum sensing mechanism in association with these nonspecific AHL signaling molecules should be further evaluated to determine their actual impact.

Our previously reported AhyI model indicated the importance of a hydrophobic ligand pocket, hydrogen bonding interactions and several crucial residues with respect to AHL synthesis. However, the molecular basis enabling AhyI to selectively recognize native acyl-ACP substrates from the cellular acyl-ACP pool has yet to be defined. As previously noted, nine hydrophobic residues (I67, L100, L103, F125, V144, I151, F152, L155, and L157) form an acyl-chain binding pocket of AhyI (Fig. S3). Indeed, similar residues have generally hydrophobic characteristics in other LuxI homologue proteins, but acyl chain size and length of native acyl-donor substrates varies. To understand the acyl-ACP substrate preference for AhyI, a structural comparison was performed for linear AHL synthases TofI (C_8-HSL), BmaI1 (C_8-HSL) and AhyI (C_4-HSL) (Fig. 5). A notable difference between the respective acyl-chain binding pockets is the replacement of small aliphatic residues (A68, L126 and V158 in TofI and BmaI1) with larger hydrophobic residues (I67, F125 and L157, respectively in AhyI), which may constrain the binding pocket in AhyI to only accommodate the shorter acyl substrates. Of these changes, the replacement of A68 with a three carbons longer I67 that with L100 are located at the bottom of the acyl-chain pocket in AhyI would likely restrict acyl chain length to C4 or C6. Notably, two key residues (i.e. L103 and V144) locate adjacent to the pocket periphery, but TofI and BmaI1 contain two larger residues F105 and T145 at the equivalent position respectively, which could influence in ligand acyl chain selection, in turn allowing AhyI to accommodate an expanded set of longer acyl group. Thus, variances at the positions provided a relatively reasonable explanation for how AhyI can recognize non-native acyl-ACP substrates (C8~C14), albeit the acyl-chain pocket volume limit. Recently, a similar tunnel prediction had been verified by the observation of the increase in C_4-HSL production and decrease in C_{12}-HSL after a corresponding residue T105Y mutation in MplI [36].

The results obtained by Dong et al. [19, 36] showed that the acyl-substrate tolerance of some CoA-based LuxI synthases is likely to depend on the volume of binding pocket, as a consequence of residues important for acyl group binding occuping the position of branched or linear alkyl-group of acyl-CoA substrates. Hence, in order to further test the relationship between the pocket size and the acyl-ACP substrate tolerance, we carried out computational alanine mutation using AutoDock program to compare the autodock-score values. Surface views of acyl-chain pocket of WT AhyI protein with six acyl-ACP substrates were shown in Fig S4. Auto dock results indicated that the relative binding affinities were increased upon introduction of mutations, excluding the replacing I67 with alanine reducing the binding affinity of C_8-ACP to the protein by 0.44 kcal/mol (Fig. 6). Notably, the binding affinities have a more remarkable increase for non-native acyl-ACPs interacting with AhyI mutations, suggested that increasing the volume of binding pocket would significantly facilitate AhyI to recognize medium-long chain acyl

substrate. However, the computational data of the ligand binding models presented in this study were insufficiency to prove the structure-function relationship, our future kinetic analysis of site-specific variants will be performed to better understand the mechanism of acyl substrate selective recognition for AhyI.

Conclusions

In this study, six linear acyl-ACP proteins with C-terminal his-tags were synthesized by *V. harveyi* AasS using the fatty acids and active holo-ACP proteins from recombinant *E. coli*. Six types of AHL molecules were specifically produced by the ACP-dependent AHL synthase AhyI through in vitro enzymatic reaction, indicating that AhyI can synthesize the short-, medium- and long-chain AHL signals using the SAM and corresponding linear acyl-ACP substrates. Kinetic studies of AhyI reacting with a panel of four linear acyl-ACPs showed a notable decrease in catalytic efficiency with increase of the acyl-chain length above C6. Hyperbolic or sigmoidal response in rate curves for varying acyl-donor substrates suggest that C_4/C_6-ACP are the native acyl-donor substrates for AhyI and others with longer linear chains than C6 are considered as non-native acyl-ACPs. Based on a structural comparison, three key hydrophobic residues (I67, F125 and L157) as part of the acyl-chain binding pocket were preliminarily proposed to be the structural determinants driving native acyl-ACP selective recognition for AhyI. The calculation data of molecular docking simulations further support this proposition by extremely increased binding affinities for non-native acyl-ACPs interacting with a representative subset of AhyI mutations. Our structural data are expected to provide theoretical direction on the molecular basis for native acyl-ACP specific recognition by AhyI.

Abbreviations

AHL, N-acyl-homoserine lactone; SAM, S-adenosyl-L-methionine; ACP, acyl carrier protein; acyl-ACP, acyl-acyl carrier protein; C_4-ACP, butyryl-ACP; C_6-ACP, hexanoyl-ACP; C_8-ACP, octanoyl-ACP; C_{10}-ACP, decanoyl-ACP; C_{12}-ACP, dodecanoyl-ACP; C_{14}-ACP, tetradecanoyl-ACP; CoA, coenzyme A; acyl-CoA, acyl-coenzyme A; C_4-HSL, N-butyryl-homoserine lactone; C_6-HSL, N-hexanoyl-homoserine lactone; C_8-HSL, N-octanoyl-homoserine lactone; C_{10}-HSL, N-decanoyl-homoserine lactone; C_{12}-HSL, N-dodecanoyl-homoserine lactone; C_{14}-HSL, N-tetradecanoyl-homoserine lactone; QS, quorum sensing; PAGE, polyacrylamide gel electrophoresis; UPLC-MS/MS, ultraperformance liquid chromatography-tandem mass spectrometry.

Declarations

Ethics approval and consent to participate

Not applicable

Consent for publication

Not applicable

Availability of data and materials

All data generated or analysed during this study are included in this published article and its supplementary information files.

Competing interests

The authors declare that they have no competing interests

Funding

No funding

Author Contributions

J.L. is the frst author on the manuscript; he completed all the experimental work and drafed the manuscript. C.Y. is the second author on the manuscript; she assisted on the AHL products analysis and prepared figure 3. Y.W.G. is the corresponding author on the manuscript; she is the project principal investigator, and performed the experimental design. All authors have read and agreed to the published version of the manuscript.

Acknowledgements

Not applicable

Supplementary Materials

The Supporting Information to this article can be found on the supplementary file.

References

1. Janda JM, Abbott SL. The genus *Aeromonas*: taxonomy, pathogenicity, and infection. Clin Microbiol Rev. 2010; *23*(1): 35–73.
2. Tomás JM. The main *Aeromonas* pathogenic factors. ISRN Microbiol. 2012; *2012*: 256261.
3. Zhang X, Yang W, Wu H, Gong X, Li A. Multilocus sequence typing revealed a clonal lineage of *Aeromonas hydrophila* caused motile *Aeromonas* septicemia outbreaks in pond-cultured cyprinid fish in an epidemic area in central China. Aquaculture. 2014; *432*: 1–6.
4. Hossain MJ, Waldbieser GC, Sun D, Capps NK, Hemstreet WB, Carlisle K, et al. Implication of lateral genetic transfer in the emergence of *Aeromonas hydrophila* isolates of epidemic outbreaks in channel catfish. PLoS One. 2013; *8*(11): e80943.

5. Stratev D, Odeyemi OA. Antimicrobial resistance of *Aeromonas hydrophila* isolated from different food sources: A mini-review. J Infect Public Heal. 2016; 9(5): 535–44.
6. Bassler BL. Small talk: cell-to-cell communication in bacteria. Cell. 2002; *109*(4): 421–24.
7. Papenfort K, Bassler BL. Quorum sensing signal-response systems in Gram-negative bacteria. Nat Rev Microbiol. 2016; *14*(9): 576–88.
8. Fuqua C, Greenberg EP. Listening in on bacteria: acyl-homoserine lactone signalling. Nat Rev Mol Cell Biol. 2002; *3*(9): 685–95.
9. Schuster M, Joseph Sexton D, Diggle SP, Peter Greenberg E. Acyl-homoserine lactone quorum sensing: from evolution to application. Annu Rev Microbiol. 2013; *67*: 43–63.
10. Helman Y, Chernin L. Silencing the mob: disrupting quorum sensing as a means to fight plant disease. Mol Plant Pathol. 2015; *16*(3): 316–29.
11. Khajanchi BK, Sha J, Kozlova EV, Erova TE, Suarez G, Sierra JC, et al. N-acylhomoserine lactones involved in quorum sensing control the type VI secretion system, biofilm formation, protease production, and in vivo virulence in a clinical isolate of *Aeromonas hydrophila*. Microbiology. 2009; *155*: 3518–31.
12. Lynch MJ, Swift S, Kirke DF, Keevil CW, Dodd CE, Williams P. The regulation of biofilm development by quorum sensing in *Aeromonas hydrophila*. Environ Microbiol. 2002; *4*(1): 18–28.
13. Swift S, Lynch MJ, Fish L, Kirke DF, Tomás JM, Stewart GS, et al. Quorum sensing-dependent regulation and blockade of exoprotease production in *Aeromonas hydrophila*. Infect Immun. 1999; *67*(10): 5192–99.
14. Vilches S, Jimenez N, Tomás JM, Merino S. *Aeromonas hydrophila* AH-3 type III secretion system expression and regulatory network. Appl Environ Microbiol. 2009; *75*(19): 6382–92.
15. Fast W, Tipton PA. The enzymes of bacterial census and censorship. Trends Biochem Sci. 2012; *37*(1): 7–14.
16. Lindemann A, Pessi G, Schaefer AL, Mattmann ME, Christensen QH, Kessler A, et al. Isovaleryl-homoserine lactone, an unusual branched-chain quorum-sensing signal from the soybean symbiont *Bradyrhizobium japonicum*. Proc Natl Acad Sci USA. 2011; *108*(40): 16765–70.
17. Moré MI, Finger LD, Stryker JL, Fuqua C, Eberhard A, Winans SC. Enzymatic synthesis of a quorum-sensing autoinducer through use of defined substrates. Science. 1996; *272*(5268): 1655–58.
18. Peres CM, Schmidt S, Juhaszova K, Sufrin JR, Harwood CS. A new class of homoserine lactone quorum-sensing signals. Nature. 2008; *454*(7204): 595–99.
19. Dong SH, Frane ND, Christensen QH, Greenberg EP, Nagarajan R, Nair SK. Molecular basis for the substrate specificity of quorum signal synthases. Proc Natl Acad Sci USA. 2017; *114*(34): 9092–97.
20. Raychaudhuri A, Tullock A, Tipton PA. Reactivity and reaction order in acylhomoserine lactone formation by *Pseudomonas aeruginosa* RhlI. Biochemistry. 2008; *47*(9): 2893–98.
21. Watson WT, Minogue TD, Val DL, von Bodman SB, Churchill ME. Structural basis and specificity of acyl-homoserine lactone signal production in bacterial quorum sensing. Mol Cell. 2002; 9(3): 685–

94.

22. Christensen QH, Brecht RM, Dudekula D, Greenberg EP, Nagarajan R. Evolution of acyl-substrate recognition by a family of acyl-homoserine lactone synthases. PLoS One. 2014; *9*(11): e112464.
23. Raychaudhuri A, Jerga A, Tipton PA. Chemical mechanism and substrate specificity of RhlI, an acylhomoserine lactone synthase from *Pseudomonas aeruginosa*. Biochemistry. 2005; *44*(8): 2974–81.
24. Gould TA, Schweizer HP, Churchill ME. Structure of the *Pseudomonas aeruginosa* acyl-homoserinelactone synthase LasI. Mol Microbiol. 2004; *53*(4): 1135–46.
25. Chung J, Goo E, Yu S, Choi O, Lee J, Kim J, et al. Small-molecule inhibitor binding to an N-acyl-homoserine lactone synthase. Proc Natl Acad Sci USA. 2011; *108*(29): 12089–94.
26. Dyda F, Klein DC, Hickman AB. GCN5-related N-acetyltransferases: a structural overview. Annu Rev Bioph Biom. 2000; *29*(1): 81–103.
27. Shin D, Gorgulla C, Boursier ME, Rexrode N, Brown EC, Arthanari H, et al. N-Acyl homoserine lactone analog modulators of the *Pseudomonas aeruginosa* RhlI quorum sensing signal synthase. ACS Chem Biol. 2019; *14*(10): 2305–14.
28. Montebello AN, Brecht RM, Turner RD, Ghali M, Pu X, Nagarajan R. Acyl-ACP substrate recognition in *Burkholderia mallei* BmaI1 acyl-homoserine lactone synthase. Biochemistry. 2014; *53*(39): 6231–42.
29. Jin L, Chen Y, Yang W, Qiao Z, Zhang X. Complete genome sequence of fish-pathogenic *Aeromonas hydrophila* HX-3 and a comparative analysis: insights into virulence factors and quorum sensing. Sci Rep-UK. 2020; *10*(1): 1–15.
30. Swift S, Karlyshev AV, Fish L, Durant EL, Winson MK, Chhabra SR, et al. Quorum sensing in *Aeromonas hydrophila* and *Aeromonas salmonicida*: identification of the LuxRI homologs AhyRI and AsaRI and their cognate N-acylhomoserine lactone signal molecules. J Bacterial. 1997; *179*(17): 5271–81.
31. Jin L, Zhang X, Shi H, Wang W, Qiao Z, Yang W, et al. Identification of a Novel N-Acyl Homoserine Lactone Synthase, AhyI, in *Aeromonas hydrophila* and Structural Basis for Its Substrate Specificity. J Agr Food Chem. 2020; *68*(8): 2516–27.
32. Rock CO, Jackowski S. Forty years of bacterial fatty acid synthesis. Biochem Bioph Res Co. 2002; *292*(5): 1155–66.
33. Thomas J, Cronan JE. The enigmatic acyl carrier protein phosphodiesterase of *Escherichia coli*: genetic and enzymological characterization. J Biol Chem. 2005; *280*(41): 34675–83.
34. Keating DH, Carey MR, Cronan Jr JE. The unmodified (apo) form of *Escherichia coli* acyl carrier protein is a potent inhibitor of cell growth. J Biol Chem. 1995; *270*(38): 22229–35.
35. Finking R, Solsbacher J, Konz D, Schobert M, Schäfer A, Jahn D, et al. Characterization of a new type of phosphopantetheinyl transferase for fatty acid and siderophore synthesis in *Pseudomonas aeruginosa*. J Biol Chem. 2002; *277*(52): 50293–302.

36. Dong SH, Nhu-Lam M, Nagarajan R, Nair SK. Structure-Guided Biochemical Analysis of Quorum Signal Synthase Specificities. ACS Chem Biol. 2020; *15*(6): 1497–1504.
37. Wang L, Yang J, Huang C, Wang H. Overexpression and purification of *Escherichia coli* holo-acyl carrier protein and synthesis of acyl carrier protein. Acta Microbiol Sinica. 2008; *48*(7): 963–69.
38. Rock CO, Cronan Jr JE. Improved purification of acyl carrier protein. Anal Biochem. 1980; *102*(2): 362–64.
39. Jiang Y, Chan CH, Cronan JE. The soluble acyl-acyl carrier protein synthetase of *Vibrio harveyi* B392 is a member of the medium chain acyl-CoA synthetase family. Biochemistry. 2006; *45*(33): 10008–19.
40. Cronan JE, Thomas J. Bacterial fatty acid synthesis and its relationships with polyketide synthetic pathways. Method Enzymol. 2009; *459*: 395–433.
41. Christensen QH, Grove TL, Booker SJ, Greenberg EP. A high-throughput screen for quorum-sensing inhibitors that target acyl-homoserine lactone synthases. Proc Natl Acad Sci USA. 2013; *110*(34): 13815–20.
42. Morris GM, Huey R, Lindstrom W, Sanner MF, Belew RK, Goodsell DS, et al. AutoDock4 and AutoDockTools4: Automated docking with selective receptor flexibility. J Comput Chem. 2009; *30*(16): 2785–91.

Tables

Table 1. Kinetic constants for variable acyl-ACP substrates reacting with AhyI

variable acyl-ACPs	k_{cat} (s^{-1}) x 10^{-3}	K_m (M) x 10^{-6}	k_{cat}/K_m ($M^{-1}s^{-1}$) x 10^{3}	relative ratio[a]
C4-ACP	22.73 ± 3.2	1.85 ± 0.16	12.29 ± 1.61	1
C6-ACP	19.44 ± 2.4	13.18 ± 1.9	1.48 ± 0.13	0.12
C8-ACP	8.41 ± 0.79	41.37 ± 8.9	0.20 ± 0.05	0.016
C10-ACP	6.34 ± 0.43	91.79 ± 15.5	0.07 ± 0.01	0.0057

Figures

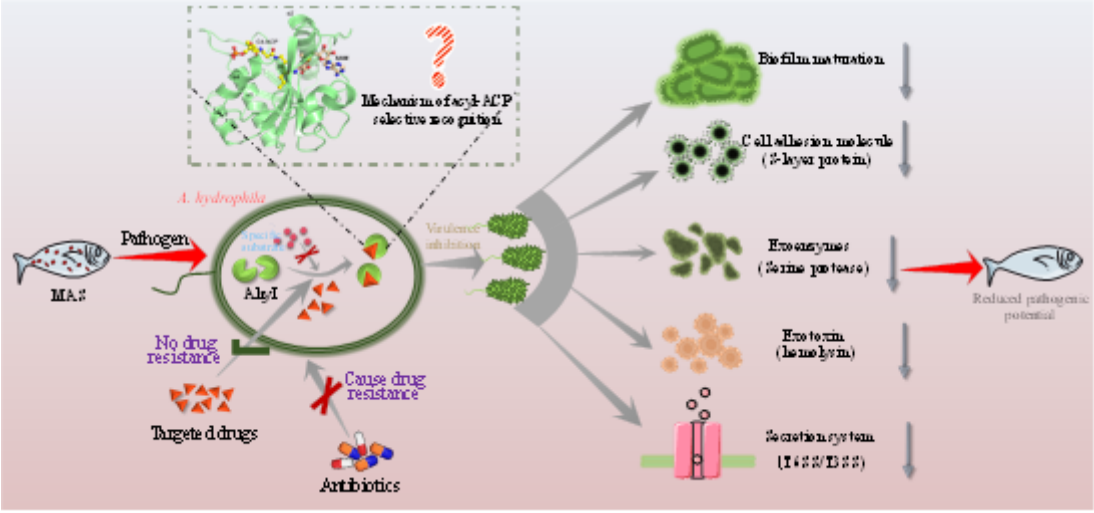

Figure 1

Schematic diagram of biocontrol and prevention of MAS disease caused by A. hydrophila using AHL-QS target-specific agents.

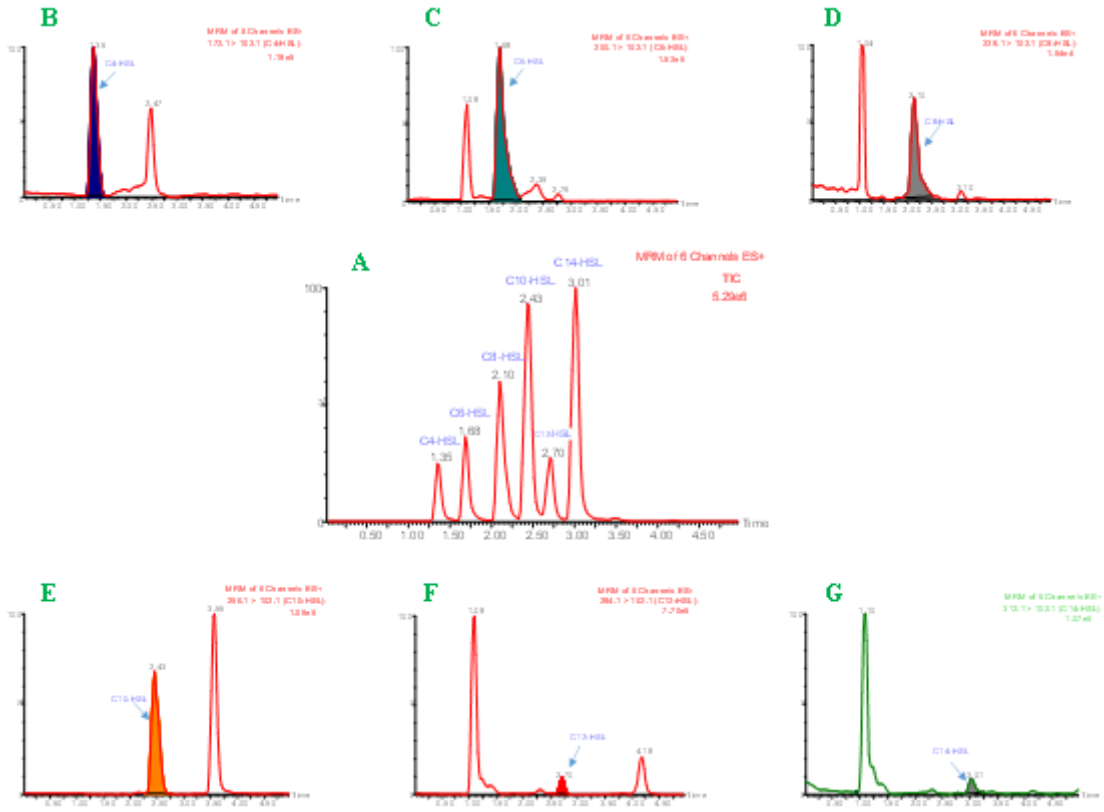

Figure 2

Typical UPLC-MS/MS ESI+ chromatograms from the AHL standard solutions (A) and in vitro enzyme reaction extracts, matching the retention times of all six AHLs, i.e., 1.35 min for C4-HSL (B), 1.68 min for C6-HSL (C), 2.10 min for C8-HSL (D), 2.43 min for C10-HSL (E), 2.70 min for C12-HSL (F) and 3.01 min for C14-HSL (G).

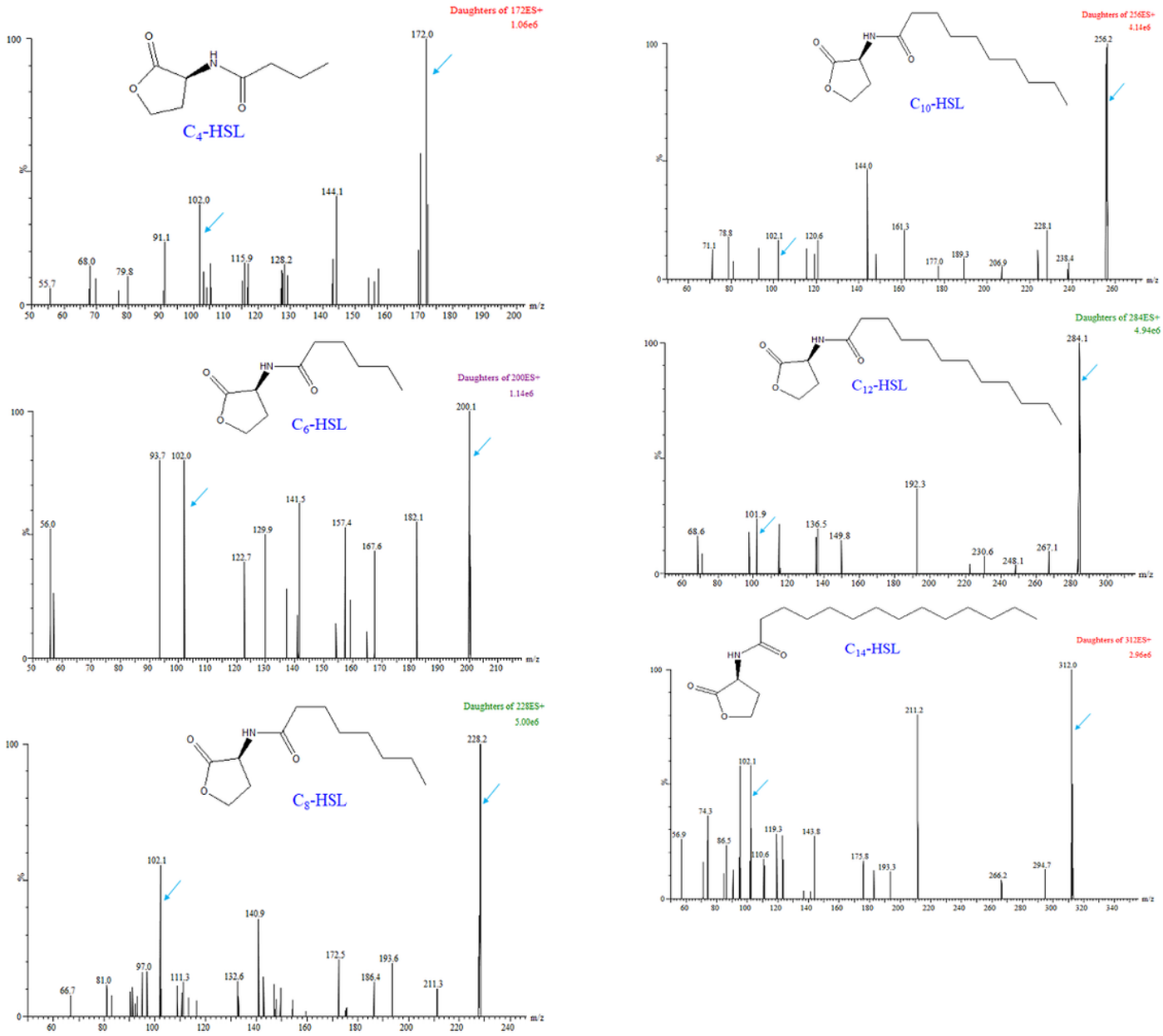

Figure 3

Mass spectra of six AHL products synthesized by AhyI via an in vitro enzymatic reaction. The characteristic peaks for respective C4-HSL (m/z 172.0→102.0), C6-HSL (m/z 200.1→102.0), C8-HSL (m/z 228.2→102.1), C10-HSL (m/z 256.2→102.1), C12-HSL (m/z 284.1→101.9) and C14-HSL (m/z 312.0→102.1) are marked by arrows.

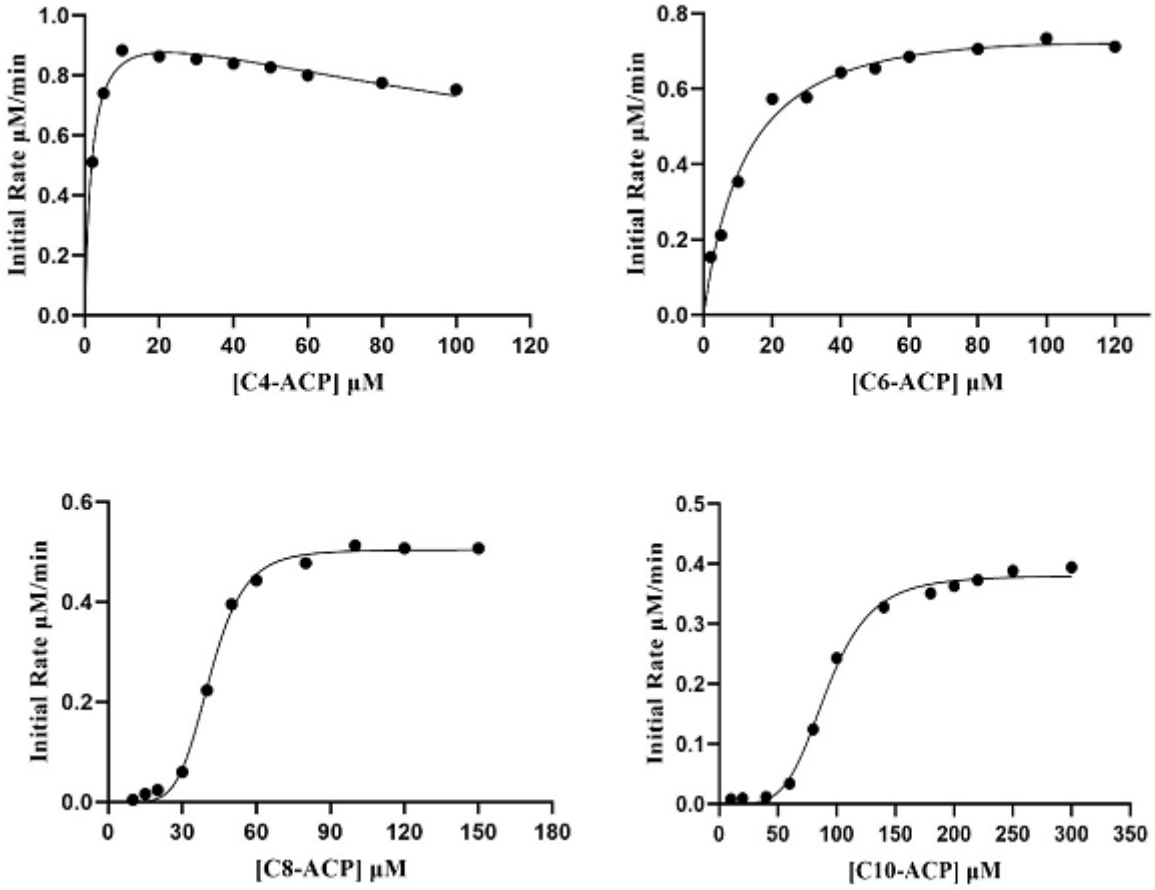

Figure 4

Substrate-velocity curves of AhyI with varying concentrations of acyl-ACPs. SAM was a fixed substrate at 1 mM, and enzyme concentrations were maintained at 0.75 μM (C4-ACP and C6-ACP) or 1 μM (C8-ACP and C10-ACP) in these experiments.

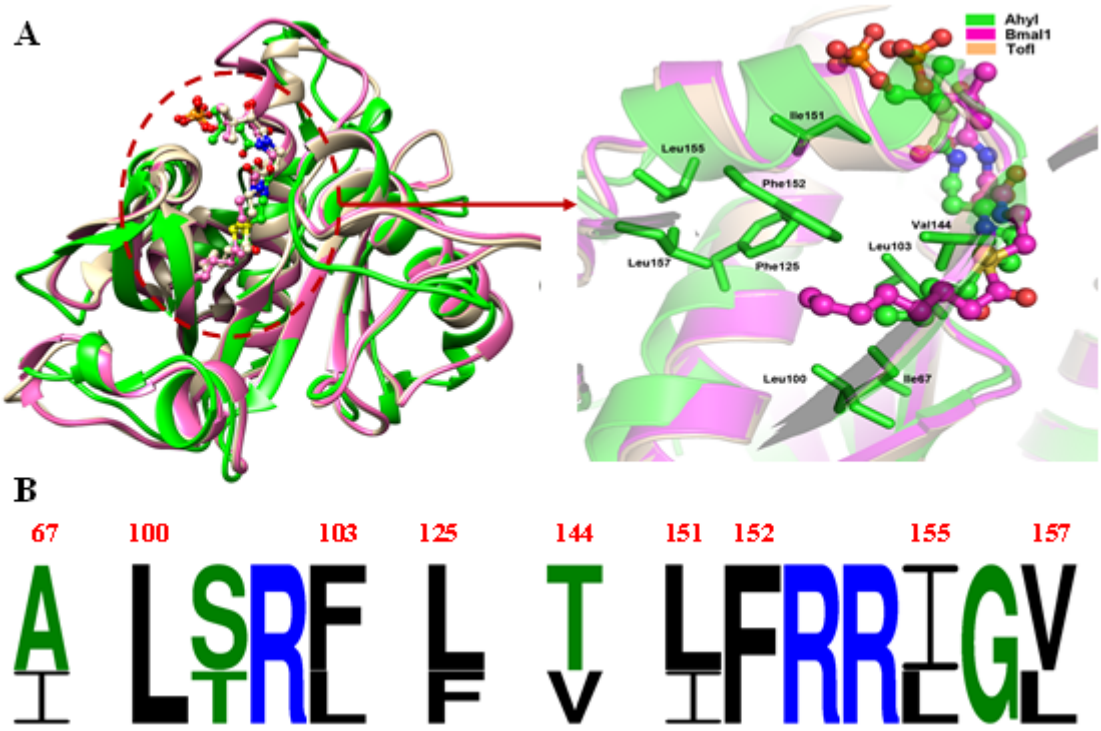

Figure 5

The structural alignment of TofI, BmaI1 and AhyI. (A) Overlapping ribbon diagram (left) of three linear AHL synthases in complex with respective native acyl substrates C8 (in pink) and C4 (in green). The closeup view (right) of acyl-chain binding pockets, with AhyI residues shown in sticks and colored in green. (B) Comparison of position-specific amino acid composition of acyl-chain binding sites based on WebLogo frequency plots, with the numbers indicating the AhyI residues.

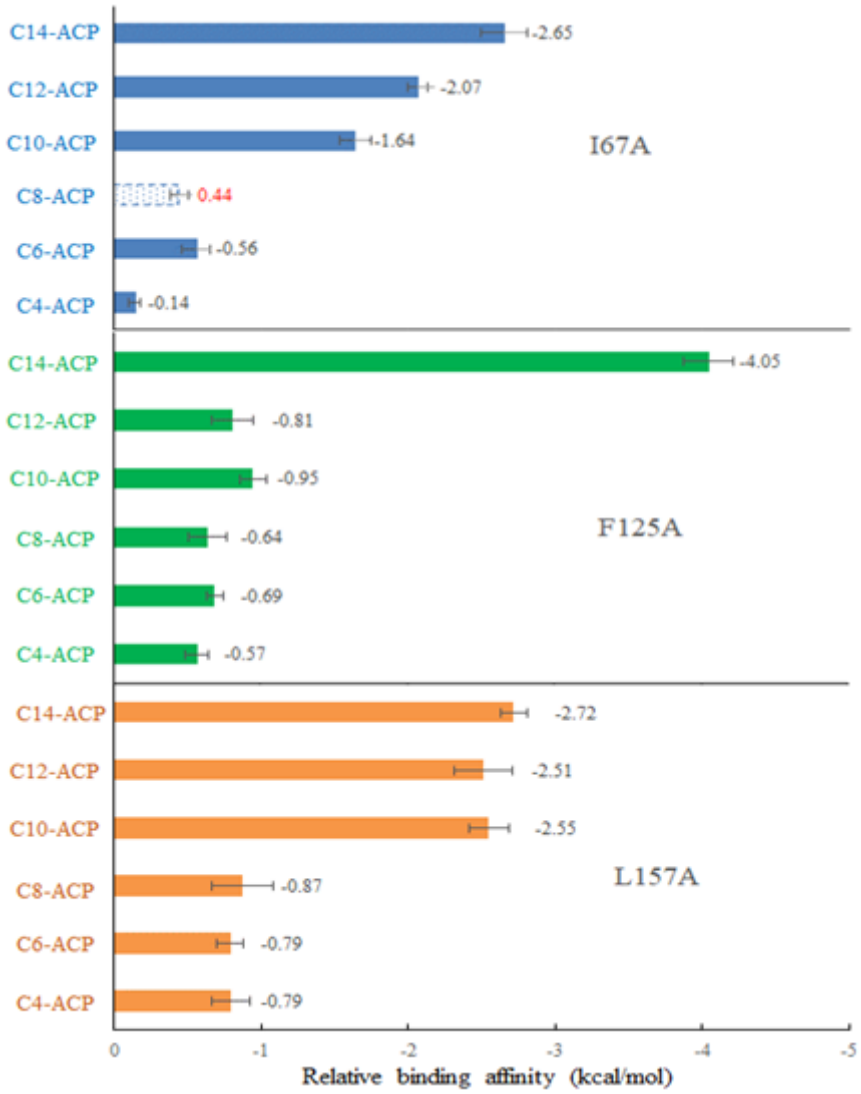

Figure 6

The relative (to WT) binding affinity obtained by docking acyl-4'-PP group of six acyl-ACP substrates into the binding pocket of wild-type (WT) AhyI or mutations. Blue dotted box with positive value colored red showed in the negative axis window, indicates the decrease in binding affinity.

Supplementary Files

This is a list of supplementary files associated with this preprint. Click to download.

- Supportingmaterial.docx